Mutation of a single residue in the ba_3 oxidase specifically impairs protonation of the pump site

Christoph von Ballmoos[#1,2], Nathalie Gonska[#2], Peter Lachmann[#3], Robert B. Gennis[4], Pia Ädelroth[2] and Peter Brzezinski[2*]

[1] Present address: Department of Chemistry and Biochemistry, University of Bern, Freiestrasse 3, 3012 Bern, Switzerland

[2] Department of Biochemistry and Biophysics, The Arrhenius Laboratories for Natural Sciences, Stockholm University, SE-106 91 Stockholm, Sweden.

[3] Present address: Applied Photophysics Ltd, 21 Mole Business Park, Leatherhead, Surrey, KT22 7BA, United Kingdom

[4] Department of Biochemistry, University of Illinois, Urbana, IL 61801, USA.

Key words: cytochrome *c* oxidase, electron transfer, membrane protein, respiration, electrochemical potential, redox reaction, metalloprotein, cytochrome aa_3.

Abbreviations: Cyt*c*O, cytochrome *c* oxidase; *n* side, negative side of the membrane; *p* side, positive side of the membrane; **R**, the four-electron reduced Cyt*c*O; **A**, reduced Cyt*c*O with O_2 bound to heme a_3; $\mathbf{P_R}$, the "peroxy" state formed after transfer of a third electron to the catalytic site; **F**, the ferryl state formed at the catalytic site after protonation of $\mathbf{P_R}$; **O**, the oxidized Cyt*c*O; DDM, n-Dodecyl β-D-maltoside.

[*] Correspondence: peterb@dbb.su.se, fax: +46-8-153679, phone +46 70 609 2642

[#] These authors have contributed equally.

source: http://boris.unibe.ch/65883/ | downloaded: 13.3.2017

Abstract

The *ba*$_3$-type cytochrome *c* oxidase from *Thermus thermophilus* is a membrane-bound protein complex that couples electron transfer to O_2 to proton translocation across the membrane. To elucidate the mechanism of the redox-driven proton pumping, we investigated the kinetics of electron and proton transfer in a structural variant of the *ba*$_3$ oxidase where a putative "pump site" was modified by replacement of Asp372 by Ile. In this structural variant proton pumping was uncoupled from internal electron transfer and O_2 reduction. The results from our studies show that proton uptake to the pump site (time constant ~65 μs in the wild-type cytochrome *c* oxidase) was impaired in the Asp372Ile variant. Furthermore, a reaction step that in the wild-type cytochrome *c* oxidase is linked to simultaneous proton uptake and release with a time constant of ~1.2 ms, was slowed to ~8.4 ms, and in Asp372Ile only associated with proton uptake to the catalytic site. These data identify reaction steps that are associated with protonation and deprotonation of the pump site and point to the area around the Asp372 as the location of this site in the *ba*$_3$ cytochrome *c* oxidase.

\body

Introduction

The heme-copper oxygen reductases are membrane-bound proteins in which the reduction of O_2 to H_2O drives proton pumping, from the negative (*n*) to the positive (*p*) side, across the membrane. The free energy from the O_2-reduction reaction, conserved in the proton gradient, is used for example for transmembrane transport and ATP synthesis. A major fraction of the oxidases known to date can be classified as members of one of three families denoted by letters A, B and C {Pereira, 2001 #2611; Hemp, 2008 #3285; Lee, 2012 #3546}. The A family includes the mitochondrial Cyt*c*O as well as the well-studied aa_3-type Cyt*c*O from *Rhodobacter* (*R.*) *sphaeroides*. These enzymes harbor four redox-active metal sites; Cu_A, the primary electron acceptor from water-soluble cytochrome *c*, as well as the intermediate electron acceptor, heme *a* and the catalytic site. The latter consists of heme a_3 and Cu_B in close proximity (for review of the structure and function of oxidases, see {Hosler, 2006 #3193; Yoshikawa, 2006 #3292; Brzezinski, 2008 #3243; Brzezinski, 2006 #3185; Ferguson-Miller, 2012 #3514; Rich, 2013 #3575; Kaila, 2010 #3460; Lee, 2012 #3546}). The A-family bacterial oxidases harbor two functional proton pathways leading from the *n* side surface toward the catalytic site. The K pathway is used for transfer of substrate protons from the *n*-side solution to the catalytic site during reduction of the catalytic site, while the D pathway is used for transfer of the remaining substrate protons and all pumped protons after binding of O_2 at the catalytic site (the K pathway is not used after O_2 binding {Svahn, 2014 #3772}).

The most studied member of the B family is the ba_3 Cyt*c*O from *Thermus* (*T.*) *thermophilus* in which the intermediate electron acceptor is heme *b* instead of heme *a* {Soulimane, 2000 #2460; Tiefenbrunn, 2011 #3572; Luna, 2008 #3438} (**Figure 1a**). As presumably other members of the B-family, the ba_3 Cyt*c*O uses only one proton pathway for transfer of all substrate protons as well as protons that are pumped across the membrane {Chang, 2009 #3286}. This pathway overlaps in space with the K pathway of the A oxidases and therefore it is referred to as the K pathway analogue. While the A-type oxidases studied to date typically pump ~1 H^+ per electron transferred to O_2, the B-type oxidases display a lower stoichiometry of ~0.5 H^+/e^- {Siletsky, 2007 #3221; Kannt, 1998 #2279; Han, 2011 #3464}.

Proton pumping against an electrochemical gradient across the membrane requires a protonatable site with alternating access to the two sides of the membrane. This site, often referred to as the "proton-loading site", PLS, would initially become protonated specifically from the *n* side (but not the *p* side) and then release its proton to the *p* side (but not the *n* side) {Popović, 2004 #3006; Quenneville, 2006 #3155; Sharpe, 2008 #3320; Blomberg, 2012 #3515; Kaila, 2011 #3596; Johansson, 2011 #3481;Chakrabarty, 2011 #3442;Olsson, 2006 #3175}. The identity of the PLS of the heme-copper oxidases is not known. Nevertheless, assuming that this site is common to all members of the heme-copper oxidase superfamily there is a limited number of candidates such as e.g. propionates A or/and D of heme a_3, possibly including surrounding water molecules {Blomberg, 2012 #3515; Chang, 2012 #3598; Chang, 2009 #3286; Wikström, 2007 #3203; Kaila, 2011 #3596; Fee, 2008 #3436; Goyal, 2013 #3597} (see **Figure 1**). For the ba_3 Cyt*c*O, theoretical and experimental data, together with structural analyses suggest that the ring A propionate of heme a_3, including nearby sites, may act as the PLS {Chang, 2009 #3286; Chang, 2012 #3598;Koutsoupakis, 2004 #3600;Fee, 2008 #3436; Soulimane, 2000 #2460}{Koutsoupakis, 2003 #3599}. Results from a more recent study showed that structural perturbations near the heme a_3 propionate A resulted in uncoupling of proton pumping from O_2 reduction. One particularly interesting case is the replacement of Asp372 by Ile, which yielded 50% active Cyt*c*O in which proton pumping was uncoupled from O_2 reduction {Chang, 2012 #3598}. Furthermore, a detailed analysis of electrostatic interactions within a cluster of amino-acid residues around the heme a_3 propionates of several oxidases (although this study did not include the ba_3 Cyt*c*O) suggests that a cluster of residues, together with the heme a_3 propionic acids may collectively bind protons {Lu, 2014 #3773}. This cluster includes residues equivalent to Asp372 in the ba_3 Cyt*c*O (**Figure 1**).

The reaction of the four-electron reduced ba_3 Cyt*c*O with O_2 has been studied using time resolved spectroscopy after flash photolysis of the blocking CO ligand from heme a_3 at the catalytic site. The sequence of events observed with the ba_3 Cyt*c*O differs slightly from that observed with the aa_3 oxidases {Smirnova, 2013 #3745;von Ballmoos, 2012 #3760;Von Ballmoos, 2012 #3544;Von Ballmoos, 2011 #3462;Siletsky, 2007 #3221} (**Figure 2**). In both the aa_3 (here data with the *R. sphaeroides* aa_3-type Cyt*c*O are discussed) and ba_3 oxidases at neutral pH, O_2 binds initially to the reduced heme a_3 (state $\mathbf{R^2}$, the superscript denotes the number of electrons at the catalytic site) with a time

constant of ~8 μs (at 1 mM O_2) forming a state that is denoted $\mathbf{A^2}$. After binding of O_2 an electron is transferred from heme *b* to the catalytic site with a time constant of ~40 μs or ~15 μs in the *aa*$_3$ and *ba*$_3$ Cyt*c*Os, respectively, forming state $\mathbf{P^3}$ (or $\mathbf{P_R}$). In both the *aa*$_3$ and *ba*$_3$ Cyt*c*O, in the next step there is a net proton uptake from solution with time constants of ~90 μs and ~60 μs, respectively. Furthermore, the electron at Cu_A equilibrates with heme *b*/heme *a* over the same time scale, which in the *ba*$_3$ Cyt*c*O results in almost full (re-)reduction of heme *b*. However, there are also significant differences between the two oxidases. While with the *aa*$_3$ Cyt*c*O one proton is transferred to the catalytic site forming the $\mathbf{F^3}$ state and one proton is simultaneously pumped across the membrane, in the *ba*$_3$ Cyt*c*O there is only proton transfer to a site located at a distance from the catalytic site, suggested to be the PLS. The catalytic site remains in the $\mathbf{P^3}$ ($\mathbf{P_R}$) state (denoted $\mathbf{P^{3*}}$ in **Figure 2**) in the *ba*$_3$ oxidase over this time scale. With the *ba*$_3$ Cyt*c*O, in the next step a proton is transferred from solution to the catalytic site to form state $\mathbf{F^3}$ with a time constant of ~0.8 ms. This reaction approximately overlaps in time with transfer of the fourth electron, from the Cu_A - heme *b* equilibrium to the catalytic site and formation of the oxidized Cyt*c*O (state $\mathbf{O^4}$). In other words, with the *ba*$_3$ Cyt*c*O the $\mathbf{F^3}$ state is not populated at neutral pH because the $\mathbf{P^3 \rightarrow F^3}$ and $\mathbf{F^3 \rightarrow O^4}$ reactions display about the same rates (however, at higher pH (>8) the $\mathbf{F^3 \rightarrow O^4}$ reaction is slower than formation of $\mathbf{F^3}$, which allows observation of both processes, separated in time).

The data from the present study show that the initial proton uptake ($\tau \cong 65$ μs), previously interpreted to be associated with protonation of the PLS, was impaired in the Asp372Ile variant, which is the first variant displaying this behavior. Because the Asp372 residue is located "above" the catalytic site (**Figure 1**) in a protein segment that has been implied to be involved in gating of the pumped protons, the results from this study indicate a possible location of the PLS.

Results

As outlined above, carbon monoxide binds reversibly to the reduced Cyt*c*O catalytic site and the association kinetics reflects the local structure and ligand-induced structural changes. FTIR data from earlier studies of the *ba*$_3$ Cyt*c*O indicated that ligand binding to heme *a*$_3$ is linked to structural or protonation changes around Asp372 {Koutsoupakis, 2004 #3600;Koutsoupakis, 2003 #3599}. Therefore, here, we compared the kinetics of CO

recombination in the reduced wild-type and Asp372Ile variant of *ba*$_3$ Cyt*c*O from *T. thermophilus* (**Figure 3**). With the wild-type *ba*$_3$ Cyt*c*O, the increase in absorbance induced by the laser flash at *t* =0 is associated with dissociation of the CO ligand. The main component of the following absorbance decrease is associated with recombination of CO with heme *a*$_3$. As seen in **Figure 3**, the CO-recombination rate constant was ~5 s^{-1} (τ = 200 ms) which is similar to that observed earlier in an infrared study (~8 s^{-1}, {Einarsdottir, 1989 #333; Woodruff, 1993 #481}, but see also {Koutsoupakis, 2002 #3494}). With the wild-type Cyt*c*O we also observed a small, rapid component (~5 % of the total absorbance decrease) with a rate constant of ~5000 s^{-1} (τ = 200 μs), which may be associated with release of CO from Cu_B into solution (see {Von Ballmoos, 2012 #3544} and Discussion). With the Asp372Ile mutant Cyt*c*O, the rate of the rapid component decreased slightly to ~4000 s^{-1} (τ = 250 μs), but its amplitude increased significantly to ~35 % of the total absorbance change. With the Asp372Ile Cyt*c*O, the CO-recombination to heme *a*$_3$ displayed two components with rate constants of ~120 s^{-1} (25%) and 5 s^{-1} (40 %), where the latter is the same as that observed with the wild-type Cyt*c*O.

A solution of the fully reduced *ba*$_3$ Cyt*c*O with CO bound at heme *a*$_3$ was mixed with an oxygen-saturated solution in a stopped-flow apparatus (pH 7.5). The CO ligand was dissociated by a short laser flash approximately 30 ms after mixing, which allowed O_2 to bind to the catalytic site. **Figure 4** shows absorbance changes at wavelengths characteristic to redox-changes of the metal sites as well as changes in the ligation state at the catalytic site. In **Figure 4a,** the unresolved decrease in absorbance at 430 nm is associated with dissociation of the CO ligand and binding of O_2. With both the wild-type and Asp372Ile variants of Cyt*c*O this process was followed in time by an increase in absorbance with a time constant of ~15 μs associated with electron transfer from heme *b* to the catalytic site. A decrease in absorbance with the same time constant is also seen at 560 nm (**Figure 4b**) reflecting the oxidation of heme *b*. With the wild-type Cyt*c*O this decrease in absorbance at 430 nm was followed in time by an increase in absorbance with a time constant of 65 μs associated with electron transfer from Cu_A to heme *b*. With the Asp372Ile variant this increase in absorbance was not observed at 430 nm (**Figure 4a**) and it was very small at 560 nm (**Figure 4b**), which indicates that the electron transfer from Cu_A to heme *b* was impaired. The final decrease in absorbance occurred with time constants of ~1.2 ms and 8.4 ms with the wild-type and the Asp372Ile variants of Cyt*c*O,

respectively. Thus, electron transfer to the catalytic site linked to oxidation of the Asp372Ile variant of Cyt*c*O was significantly slower with Asp372Ile than with the wild-type Cyt*c*O. However, it should be noted that while with the wild-type Cyt*c*O the electron transfer occurs from heme *b*, in the Asp372Ile variant the electron is transferred from Cu_A.

At 610 nm (**Figure 4d**) the increase in absorbance with a time constant of ~15 μs is associated with electron transfer from heme *b* to the catalytic site forming state $\mathbf{P^3}$ with both the wild-type and the Asp372Ile variant of Cyt*c*O. The following decrease in absorbance is presumably associated decay of the peroxy ($\mathbf{P^3}$ or $\mathbf{P^{3*}}$) state concomitantly with formation of the ferryl ($\mathbf{F^3}$) state, which in the wild-type occurs with a time constant of ~0.8 ms. This decrease in absorbance was about a factor of two faster with the Asp372Ile mutant ($\tau \cong 0.4$ ms, **Figure 4d**) than with the wild-type Cyt*c*O ($\tau \cong 0.8$ ms).

With the wild-type ba_3 Cyt*c*O proton uptake occurs with time constants of ~65 μs and ~0.8 ms (**Figure 4c**), i.e. with the same time constants as the electron transfer from Cu_A to heme *b* and formation of the $\mathbf{F^3}$ state, respectively {Von Ballmoos, 2012 #3760;Von Ballmoos, 2012 #3544;Von Ballmoos, 2011 #3462}. However, with the Asp372Ile variant of the Cyt*c*O the fast (~65 μs) proton-uptake component was absent. Instead, two slower components were observed with time constants of ~0.4 ms and ~8.4 ms, i.e. overlapping in time with the $\mathbf{P^3 \rightarrow F^3}$ and $\mathbf{F^3 \rightarrow O^4}$ reactions, respectively (**Figure 4c**).

Figure 5a shows the pH dependence of the absorbance decrease at 610 nm in the range pH 6-10. This absorbance change reflects formation of $\mathbf{F^3}$, which was a factor of ~2 faster with the Asp372Ile variant than with the wild-type Cyt*c*O (see also above) and essentially independent of pH. **Figure 5b** shows the pH dependence of the final oxidation of the Cyt*c*O (decrease in absorbance at 560 nm). As seen in the **Figure 5b** this reaction displayed a relatively strong pH dependence for the wild-type Cyt*c*O (see {Von Ballmoos, 2012 #3544}), while with the Asp372Ile variant the reaction rate was essentially pH independent. At pH ~10 the rates with the wild-type and the Asp372Ile variants of Cyt*c*Os were about the same (~120 s^{-1}).

Discussion

Results from earlier studies using infrared spectroscopy indicated a link between ligand binding and changes in structure and/or protonation around Asp372 {Koutsoupakis, 2004 #3600;Koutsoupakis, 2003 #3599}. The CO-photolysis data in **Figure 3** support these conclusions because they show that changes in the structure at Asp372 (the Asp372Ile replacement) result in alteration of the CO-rebinding dynamics . In ba_3 variants where residues of the K-pathway analogue were altered, no such change in the CO recombination kinetics was observed (unpublished data), reinforcing the suggestion that Asp372 is linked to the catalytic site. After dissociation from heme a_3, CO binds transiently to Cu_B after which the ligand is released into solution, presumably triggered by a structural relaxation of the catalytic site {Pilet, 2004 #3331}. With the bovine heart mitochondria Cyt*c*Os {Heitbrink, 2002 #2775; Einarsdóttir, 1993 #326} and *R. sphaeroides* {Namslauer, 2002 #3671} this event gives rise to a small absorbance decrease at 445 nm with a time constant of 1-2 μs. The CO ligand binds to Cu_B also in the ba_3 oxidase {Koutsoupakis, 2002 #3494; Woodruff, 1993 #481} and the release is presumably reflected in the absorbance decrease at 445 nm after CO dissociation with a time constant of 200-250 μs {Von Ballmoos, 2012 #3544} (**Figure 3**). This event is slower than observed with the mitochondrial and *R. sphaeroides* Cyt*c*Os, but faster than the corresponding absorbance changes in the infrared region with the ba_3 Cyt*c*O ($\tau \cong 30$ ms, {Koutsoupakis, 2002 #3494}). As seen in **Figure 3** the relative amplitude of the 200-250 μs component was significantly increased with the Asp372Ile variant, which indicates that the replacement of Asp372alters the structural relaxation at the catalytic site that is linked to CO release from Cu_B.

With the A-type oxidases, after formation of state $\mathbf{P^3}$, two protons are taken up with a time constant of ~100 μs where one of the protons is transferred to the catalytic site to form state $\mathbf{F^3}$ while the other proton is presumably transferred to the PLS (**Figure 2**), and in H_2O simultaneously released to the *p* side {Salomonsson, 2005 #3161; Faxén, 2005 #2975}. With the wild-type ba_3 Cyt*c*O, the first proton, taken up with a time constant of ~65 μs, is presumably transferred to the PLS {Von Ballmoos, 2011 #3462; Von Ballmoos, 2012 #3760}. A second proton is taken up more slowly, with a time constant of ~0.8 ms, which leads to formation of state $\mathbf{F^3}$ at the catalytic site {Von Ballmoos, 2011 #3462; Smirnova, 2013 #3745; Von Ballmoos, 2012 #3760}. With the Asp372Ile ba_3 Cyt*c*O, the

initial electron transfer from heme *b* to the catalytic site (formation of **P^3**) displayed a similar time constant to that observed with the wild-type Cyt*c*O ($\tau \cong 15$ μs). However, the first proton uptake was not observed with the Asp372Ile *ba*$_3$ Cyt*c*O (**Figures 4c** and **6**). Because this structural variant does not pump protons {Chang, 2012 #3598} and in the wild-type Cyt*c*O the 65-μs proton is presumably transferred to the PLS {Von Ballmoos, 2011 #3462; Von Ballmoos, 2012 #3760}, the absence of this proton uptake supports the earlier proposals (see the Introduction section) that the PLS is located in a protein segment involving the Asp372 residue. The electron transfer from Cu$_A$ to heme *b*, which in the wild-type *ba*$_3$ Cyt*c*O is synchronized with proton uptake to PLS {Von Ballmoos, 2011 #3462}, was not observed with the Asp372Ile variant (**Figures 4** and **6**). This result is consistent with the earlier observation with the *aa*$_3$ Cyt*c*O {Karpefors, 1998 #2256} that in the wild-type Cyt*c*O the Cu$_A$ - heme *b* electron transfer is induced by protonation of the PLS.

In the next step of the reaction, formation of the **F^3** state, linked to proton uptake to the catalytic site, was a factor of two faster with the Asp372Ile mutant than with the wild-type Cyt*c*O (~0.4 ms and ~0.8 ms for the Asp372Ile and wild-type Cyt*c*Os, respectively). This difference may be due to a larger negative potential at the catalytic site in state **P^3** (i.e. after electron transfer from heme *b* to the catalytic site) in the mutant Cyt*c*O because of the absence of a proton at the PLS.

The **F^3** $\rightarrow$ **O^4** reaction with the A-type oxidases is linked to proton uptake to the catalytic site and proton pumping {Verkhovsky, 1997 #2398; Faxén, 2005 #2975}. Also with the *ba*$_3$ oxidase this reaction step is linked to proton pumping {Siletsky, 2007 #3221}. However, with the wild-type *ba*$_3$ Cyt*c*O the **F^3** $\rightarrow$ **O^4** reaction is not associated with any *net* proton uptake, presumably because the proton stored at PLS is released with the same time constant as proton uptake to the catalytic site (which has to be taken up to form the oxidized state, **O^4**) {Von Ballmoos, 2011 #3462;Von Ballmoos, 2012 #3544;Von Ballmoos, 2012 #3760}. With the Asp372Ile variant, on the other hand, the **O^4** state was associated with a net proton uptake from solution (**Figure 4c**). This observation is consistent with the absence of the 65-μs proton uptake after formation of **P^3**. If the PLS does not become protonated, the **F^3** $\rightarrow$ **O^4** reaction is not associated with proton release from the PLS and only the net proton uptake to the catalytic site during formation of **O^4** is observed (see **Figure 6**).

Another difference between the Asp372Ile variant and the wild-type Cyt*c*O is that formation of the oxidized state was a factor ~7 slower in the variant. The **F^3 → O^4** reaction involves a coupled electron and proton transfer to the catalytic site, where the overall rate, k_{FO}, is determined by the fraction reduced heme a_3 in state **F^3**, α_{F^-}, (in the electron equilibrium involving Cu_A, heme *b* and the catalytic site) multiplied by the proton-transfer rate to the catalytic site, k_H {Verkhovsky, 1995 #88; Karpefors, 1998 #2256; Brändén, 2005 #3144}: $k_{FO} = \alpha_{F^-} \times k_H$. Consequently, even if the **P^3 → F^3** reaction rate is unchanged or faster (c.f. value of k_H), the **F^3 → O^4** rate may be slowed if α_{F^-} is diminished, as was observed earlier with a structural variant of the *R. sphaeroides* aa_3 oxidase {Karpefors, 1998 #2256}. With the wild-type ba_3 Cyt*c*O, upon formation of state **F^3**, heme *b* is essentially fully (re-)reduced such that during **F^3 → O^4** the "fourth" electron is transferred directly from heme *b*. In the Asp372Ile structural variant, on the other hand, in state **F^3** the electron equilibrium is shifted away from heme *b* (only a small fraction heme *b* is (re-)reduced (**Figure 4ab**), which indicates that the heme *b* apparent midpoint potential in the transiently formed **F^3** state is lower than in the wild type Cyt*c*O. This difference is attributed to the unprotonated PLS in state **F^3**. Because amino-acid residue 372 is located even closer to heme a_3/Cu_B than to heme *b*, a similar decrease in the apparent midpoint potential is expected for the catalytic site in the **F^3** state As a result, during the **F^3 → O^4** reaction the fraction reduced catalytic site, α_{F^-} (see above), would be smaller with the Asp372Ile variant than with the wild-type Cyt*c*O, which would result in a slower **F^3 → O^4** reaction even though proton transfer to the catalytic site (c.f. the **P^3 → F^3** reaction) is accelerated by a factor of two.

Another reason for the slowed **F^3 → O^4** reaction with the Asp372Ile variant may be an effect on changes in structure around the K pathway and the catalytic site. Such changes in structure are required for gating the unidirectional flow of protons and must also involve the PLS (defined as a site that is alternately exposed either to the *n* or *p* side of the membrane) and are likely to modulate the proton-transfer rate through the K pathway. Consequently, it is likely that a structural modification near or at the PLS would alter the proton-transfer rate through the K pathway (c.f. also the slightly faster **P^3 → F^3** reaction discussed above).

With the wild-type *ba*$_3$ Cyt*c*O, the $\mathbf{F^3 \rightarrow O^4}$ reaction rate is pH dependent and drops by about a factor of 10 from pH 6 to 10. In contrast, with the Asp372Ile oxidase this rate was essentially pH-independent (**Figure 5**). With the wild-type *ba*$_3$ Cyt*c*O the reactions that occur before $\mathbf{P^3 \rightarrow F^3}$, i.e. proton uptake to the PLS ($\tau \cong 65\mu s$) and proton uptake to form state $\mathbf{F^3}$ ($\tau \cong 0.8$ ms), display essentially pH-independent kinetics (a decrease by a factor of ~2 over 5 pH units, {Von Ballmoos, 2011 #3462}). The unique feature of the $\mathbf{F^3 \rightarrow O^4}$ reaction with the wild-type Cyt*c*O is that it is linked to the release of a pumped proton. Consequently, the pH dependence of the $\mathbf{F^3 \rightarrow O^4}$ reaction could be associated with deprotonation of the PLS or changes in structure that are linked to this reaction. The decrease in the $\mathbf{F^3 \rightarrow O^4}$ rate with increasing pH would then reflect the degree of protonation of the PLS. Based on our data, we speculate that with the Asp372Ile variant the PLS is always deprotonated and therefore the $\mathbf{F^3 \rightarrow O^4}$ rate is approximately the same as that for the fully deprotonated PLS with the wild-type Cyt*c*O (i.e. at high pH).

Earlier FTIR spectroscopy data suggested that a possible acceptor for pumped protons is a cluster involving Asp372, a water molecule and the ring A propionate of heme *a*$_3$ {Koutsoupakis, 2004 #3600}. The same protein segment was suggested on the basis of theoretical calculations, which indicated that His376, that is also hydrogen-bonded to the ring A propionate may accept protons from the *n*-side of the membrane {Fee, 2008 #3436}. Moreover, proton pumping may also involve a water molecule bridging the heme *a*$_3$ D and A propionates {Daskalakis, 2011 #3774; Chang, 2009 #3286; Chang, 2012 #3598}, which, together with the Cu$_B$ ligand His283, was implied to be the PLS. These conclusions were also supported by data from studies of the structural variants His376Asn and Asp372Ile (investigated here), which display a significant O_2-reduction activity that is uncoupled from proton pumping {Chang, 2012 #3598}. However, the results from the same study also showed that that the uncoupling is specific to certain replacements and not to the replacement position. For example, upon replacement of His376 by Phe or Asp372 by Val proton pumping was maintained. Seemingly inconclusive results were also obtained with structural variants at the position equivalent to the *ba*$_3$ Cyt*c*O Asp372 from other organisms. With the *R. sphaeroides aa*$_3$ Cyt*c*O the effect of replacement of Asp407 by Ala, Asn or Cys was studied and the data suggested that the residue has no role in proton pumping {Qian, 1997 #412}. Similar results were obtained with the *bo*$_3$ quinol oxidase {Thomas, 1993 #1472}. With the *P. denitrificans*

Cyt*c*O the Asp399Leu replacement displayed an activity of 7 % of that of the wild-type Cyt*c*O and no proton pumping. However, with the Asp399Asn replacement the activity was ~60 % and no effect on proton pumping was observed {Pfitzner, 2000 #2463}. Collectively, these results, together with those discussed above for the *ba*$_3$ Cyt*c*O, indicate that structural changes around propionate A of heme a_3 can result in uncoupling of proton pumping, while maintaining a significant fraction of the O_2-reduction activity. However, on the basis of these studies, no unique structural elements could be identified as the PLS of the heme-copper oxidases. Furthermore, not all of these modified residues are conserved among the heme-copper oxidases. These observations support the proposal that a cluster consisting of a number of amino acid residues, water molecules and propionates A and D of heme a_3, together act as a PLS {Chang, 2012 #3598;Chang, 2009 #3286;Daskalakis, 2011 #3774}. In a recent study continuum electrostatics simulations with different *aa*$_3$ Cyt*c*O crystal structures were used to show that the PLS is not a single site, but rather includes a large number of sites, which interact with the heme a_3 propionates {Lu, 2014 #3773}. The pK_as and changes in these values determine the protonation state of the PLS. If the pK_as of the propionates are sufficiently low, the PLS does not become protonated and the Cyt*c*O would reduce O_2 to water, but without linking this reaction to proton pumping (i.e. proton pumping is uncoupled from O_2 reduction) {Lu, 2014 #3773}. The contribution of the different residues of the PLS to its net protonation state depends on the composition of the PLS and therefore varies between Cyt*c*Os from different organisms. In other words, the position of the PLS would be the same in all oxidases, but its composition would be different and be fine tuned for each structure. Consequently, the effects of mutations are likely to be different.

One way to accomplish transmembrane proton translocation in Cyt*c*O is to couple changes in the alternating proton access of the PLS to the *n* and *p* sides, respectively, to changes in its collective pK_a {Wikström, 1981 #2872}. A transmembrane proton electrochemical gradient of 180 mV is approximately equal to the free energy required to shift the pK_a of this group by 3 units. Consequently, to accomplish unidirectional proton pumping across the membrane, a PLS that conserves the free energy of the Cyt*c*O catalytic reaction should have a ΔpK_a ($pK_{a,n}$ - $pK_{a,p}$) >3 (the upper limit is the available free energy provided by oxidation of cytochrome *c* linked to reduction of O_2 to H_2O). Structural modifications within the PLS would typically result in changes in the values of $pK_{a,n}$, $pK_{a,p}$ and ΔpK_a, but changes in the protonation and deprotonation of the PLS would

depend on the values of these parameters relative to the pH and the transmembrane proton electrochemical gradient. Consequently, different structural modifications at a specific site or region may render very different effects on the pumping stoichiometry (see above). Furthermore, the requirement to protonate and deprotonate the PLS in the input and output states, respectively (i.e. the relative values of $pK_{a,n}/pH_n$ and $pK_{a,p}/pH_p$ as outlined above), may be fulfilled only in the absence of a transmembrane electrochemical potential or with a small potential *in vitro*, but not with the *in vivo* potential of the living cell.

In this context, we note that in the wild-type ba_3 oxidase there is a delay between proton uptake to the PLS ($\tau \cong 65\mu s$) and release from the PLS ($\tau \cong 1.2$ ms), which means that the PLS is protonated in the time between these events. Thus, absence of the 65-μs component in the Asp372Ile variant indicates that the structural alteration changes the properties (e.g. pK_as, see above) of the PLS itself such that it can not be protonated or it significantly slows proton transfer to the PLS. Furthermore, it is unlikely that the cause for uncoupling is a proton leak from the membrane positive side {Chang, 2012 #3598} because such a leak would be manifested as a proton uptake from solution in our experiments. Furthermore, it is unlikely that the structural alteration slows proton transfer through the exit pathway (see {Popovic, 2005 #3137}) because we would then expect to see proton uptake from solution, even if the proton would eventually be transferred "back" to the catalytic site.

In summary, the data from the present study show that the uncoupling of the proton pump is caused by slowed protonation of the PLS. Furthermore, the data point to a general location of the pump site (PLS) in the Cyt*c*O and allowed us to identify a specific reaction step in the sequence of electron and proton-transfer events that is associated with protonation of the PLS.

Materials and Methods

His-tagged wild type *ba*$_3$ Cyt*c*O was expressed and purified as described previously {Von Ballmoos, 2011 #3462}, and kept at 4°C in 5 mM Hepes, pH 7.4, 0.05% dodecyl-β-D-maltoside (DDM, Glycon, Germany).

For the flow-flash measurements a sample containing *ba*$_3$ Cyt*c*O (~5 μM Cyt*c*O in 2 mM Hepes, pH 7.4, 0.05% DDM) was transferred to an anaerobic cuvette and air was exchanged for N_2 on a vacuum line. The Cyt*c*O was reduced upon adding 0.5 μM PMS and 2 mM Na-ascorbate. After incubation until full reduction of the Cyt*c*O, the atmosphere was exchanged for CO. Redox reactions and CO binding were followed spectroscopically (Cary 4000). The reaction of the reduced Cyt*c*O with O_2 was monitored spectrophotometrically using a locally modified stopped-flow apparatus (Applied Photophysics) as described in {Brändén, 2001 #2640}. Briefly, the Cyt*c*O solution (2 mM Hepes, pH 7.5, 0.05 % DDM) was mixed 1:5 with an oxygen-saturated solution (100 mM buffer (pH 6 to pH 10), 0.05 % DDM). The reaction was initiated after 30 ms by flash photolysis of the Cyt*c*O-CO complex (Nd:YAG laser Quantel: 10 ns, 532 nm, 200 mJ). Kinetic traces were recorded at specific wavelengths using a digital oscilloscope. The following buffers were used: MES (pH 6); HEPES (pH 7-8), CHES (pH 9), CAPS (pH 10). Proton uptake from solution was monitored as described in {Smirnova, 2010 #3432}. Briefly, the Cyt*c*O solution was run over a PD-10 column (GE Healthcare) where the buffer was exchanged for 150 mM KCl at pH ~7.4 in 0.05% DDM. The Cyt*c*O was then diluted in the same buffer to a concentration of ~5 μM and placed in a Thunberg cuvette (see above). The Cyt*c*O was mixed 1:5 with an unbuffered, but pH adjusted (~pH 7.4) solution containing 150 mM KCl, 0.05% DDM and 50 μM phenol red, and the absorbance changes at 575 nm detected as a function of time.

Acknowledgments

These studies were supported by grants from the Swedish Research Council (to PB, PÄ and CvB), by grant HL 16101 from the National Institutes of Health (to RBG.). CvB was supported by a fellowship from the Swiss National Science Foundation (SNF). PÄ is a Royal Swedish Academy of Sciences Research Fellow supported by a grant from the Knut and Alice Wallenberg Foundation.

References

Figure Legends

Figure 1 Structure of the *ba*$_3$ Cyt*c*O. The electron donor to the *ba*$_3$ Cyt*c*O is cyt. c^{552}, which binds near the Cu_A site. Electrons are transferred first to Cu_A and then consecutively to heme *b* and the catalytic site composed of heme a_3 and Cu_B (red line). Protons are taken up through the K-pathway analogue from the negative (*n*) side of the membrane to the catalytic site as well as to the PLS from where they are released (pumped) to the positive (*p*) side of the membrane. The location of residue Asp372, discussed in this work, is shown. (**b, c**) A close-up view of the protein segment around Asp372 where the PLS may be located. The D and A propionic acids of heme a_3 are indicated. The blue spheres are water molecules.

Figure 2 A comparison of the reaction schemes with the A- and B-type oxidases. The reaction steps observed after mixing the Cyt*c*Os with O_2 are shown, see the text for a detailed discussion. The small circles indicate the redox-active metal sites (reduced when red) and the star is the PLS (protonated in blue). The state $\mathbf{P^{3}}$* with the *ba*$_3$ Cyt*c*O is equivalent to the $\mathbf{P^{3}}$ state in wild-type Cyt*c*O, but with protonated PLS.

Figure 3 Absorbance changes after light-induced dissociation of CO from reduced *ba*$_3$ Cyt*c*O. The increase in absorbance at 445 nm after the laser flash at *t*=0 is associated with dissociation of the CO ligand. The rapid decrease in absorbance is presumably associated with transient interaction of CO with Cu_B while the slower decrease in absorbance is associated with recombination of the CO ligand with heme a_3. Experimental conditions: ~6 µM Cyt*c*O in 100 mM Hepes (pH 7.4), 0.05%

DDM, 0.1 mM EDTA; 200 μM dithionite (added to the sample after removal of O_2).

Figure 4 Absorbance changes associated with reaction of the Asp372Ile variant and wild-type *ba*$_3$ Cyt*c*O with O_2. (**a**) At 430 nm the absorbance changes are mainly associated with redox reactions at heme *b* (the initial rapid decrease at *t*=0 is associated with dissociation of CO and binding of O_2). The decrease in absorbance in the range 0-50 μs ($\tau \cong 15$ μs) is associated with oxidation of heme *b*. With the wild-type Cyt*c*O, the increase in absorbance is associated with electron transfer from Cu_A to heme *b* ($\tau \cong 65$ μs), while the final decrease is associated with oxidation of the Cyt*c*O ($\tau \cong 1.2$ ms). With the Asp372Ile variant the increase in absorbance is not seen (c.f. $Cu_A \rightarrow$ heme *b* does not take place) and the electron is transferred from Cu_A to the catalytic site in the last step of the reaction ($\tau \cong 8.4$ ms) (**b**) Also at 560 nm, heme *b* primarily contributes to the absorbance changes. (**c**) Absorbance changes at 575 nm of the pH dye phenol red. An increase in absorbance corresponds to proton uptake from solution. (d) At 610 nm the increase in absorbance is associated with formation of the $\mathbf{P^3}$ ($\mathbf{P_R}$) state ($\tau \cong 15$ μs), while the decrease in absorbance is associated with decay of $\mathbf{P^3}$ and formation of state $\mathbf{F^3}$ ($\tau \cong 0.8$ ms and 0.4 ms with the wild-type and Asp372Ile variant Cyt*c*O). Experimental conditions: ~1 μM Cyt*c*O in 100 mM Hepes (pH 7.4), 0.05% DDM, except in (c) where the buffer was replaced with 150 mM KCl and 50 μM phenol red was added.

Figure 5 pH dependence of the F^3 and O^4 formation rates. The rate constants were obtained from absorbance changes at 610 nm (panel (**a**), decrease associated with decay of $\mathbf{P^3}$) and at 560 nm (panel (**b**), decrease associated with oxidation of the Cyt*c*O). For experimental conditions, see the Materials and Methods section.

Figure 6 Summary of results. A comparison of reaction steps linked to proton uptake observed with the wild-type and Asp372Ile *ba*$_3$ Cyt*c*Os.

Table

Table 1 Time constants associated with reaction of the reduced wild-type and Asp372Ile and O_2 at pH 7.5. Each experiment was repeated 2-15 times with 3 different samples. The standard error in the time constants was <20 %.

reaction	wild-type	Asp372Ile
heme *b* → catalytic site (**$A^2 \rightarrow P^3$**)	15μs	15μs
Cu_A → heme *b*	65μs	not observed
$P^3 \rightarrow F^3$	0.8 ms	0.4 ms
heme *b* → catalytic site (**$F^3 \rightarrow O^4$**)	1.2 ms	-
Cu_A → catalytic site (**$F^3 \rightarrow O^4$**)	-	8.4 ms
proton uptake (2 main components)	65μs (43%), 0.8 ms (57%)	65μs* (9%), 0.5 ms (43%), 8.4 ms (48%)

* A component with a fixed time constant of 65 μs was included to make the fit comparable to that with the wild-type Cyt*c*O.

Figure 1

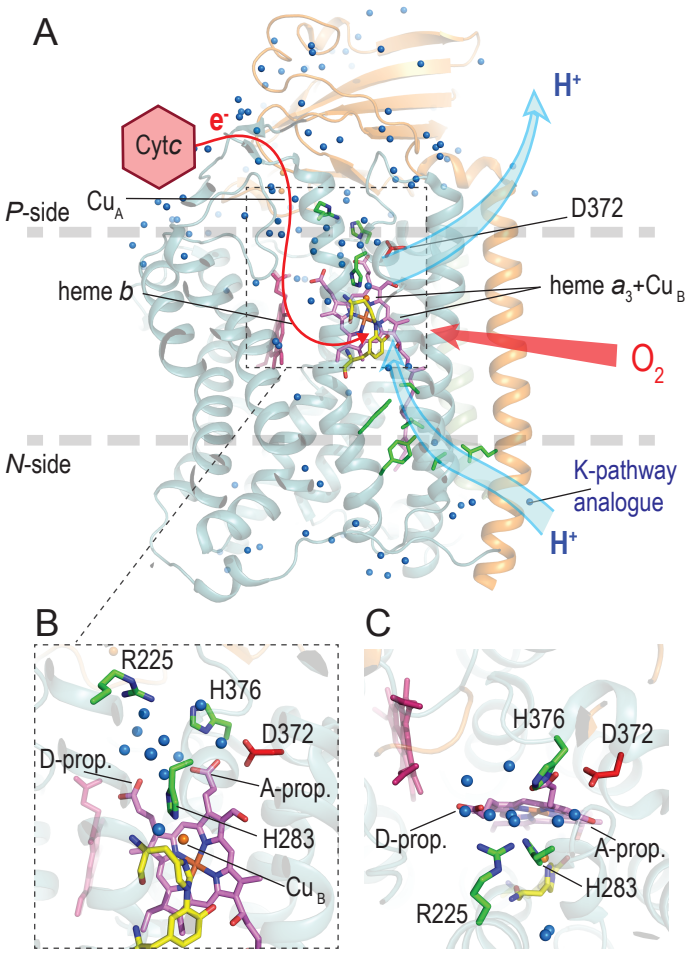
A
Cytc
e-
H+
P-side
CuA
D372
heme b
heme a3+CuB
O2
N-side
K-pathway
analogue
H+
B
R225
H376
D372
D-prop.
A-prop.
H283
CuB
C
H376
D372
D-prop.
A-prop.
H283
R225

Figure 2

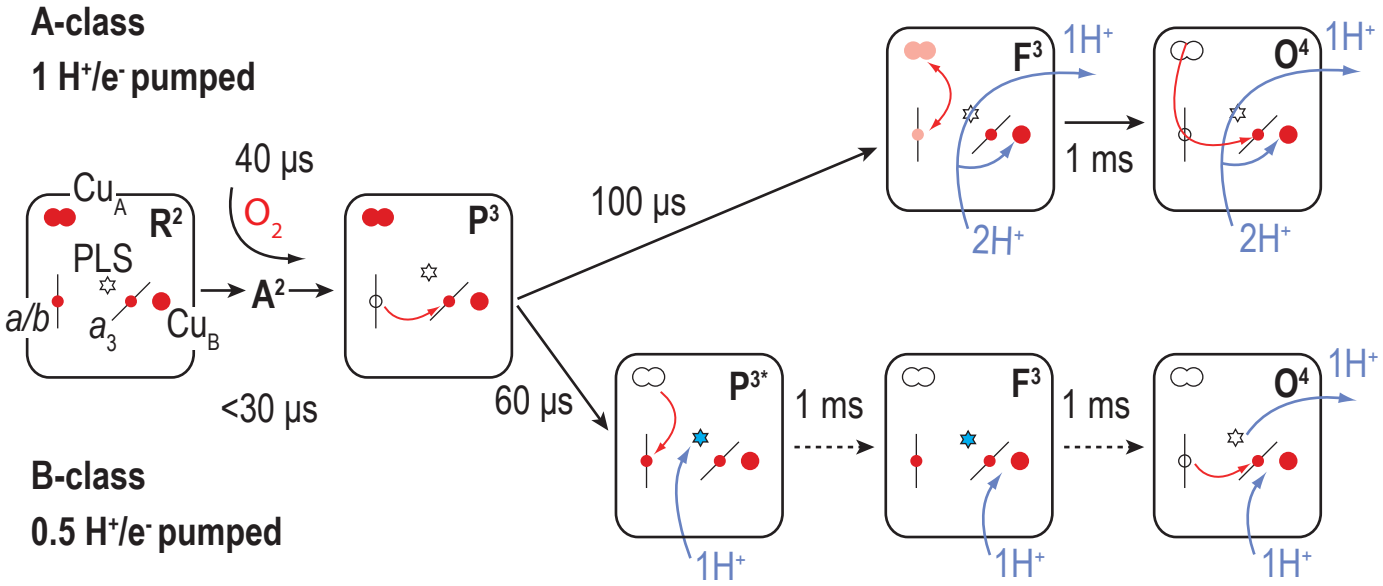
A-class
1 H+/e- pumped
CuA
R2
PLS
a/b
a3
CuB
40 µs
O2
A2
<30 µs
P3
100 µs
60 µs
F3
1H+
1 ms
2H+
O4
1H+
2H+
P3*
1 ms
F3
1 ms
O4
1H+
1H+
1H+
1H+
B-class
0.5 H+/e- pumped

Figure 3

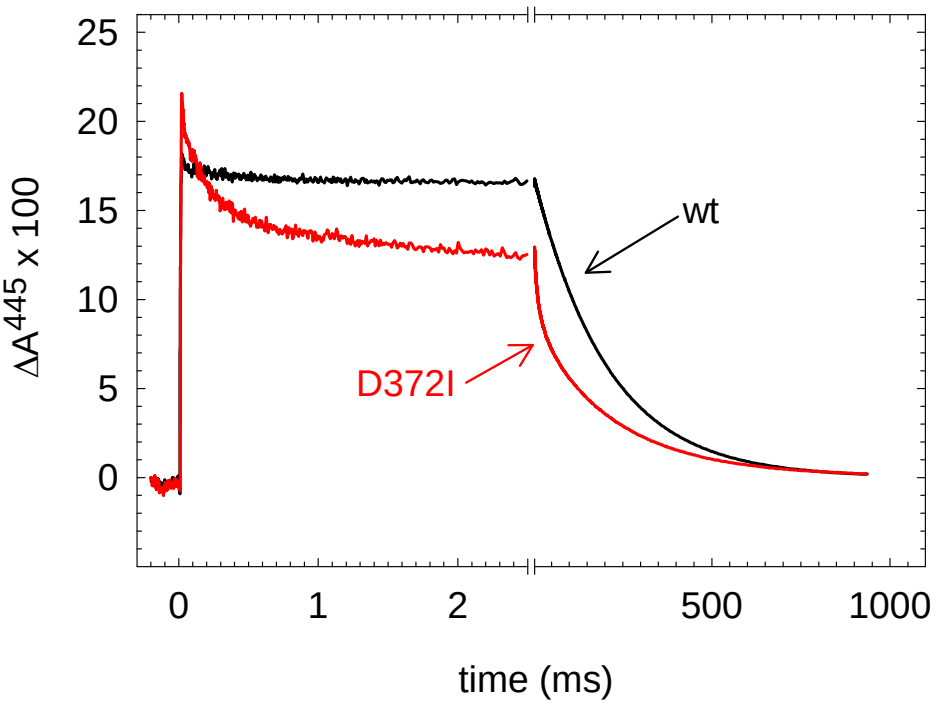

Figure 4

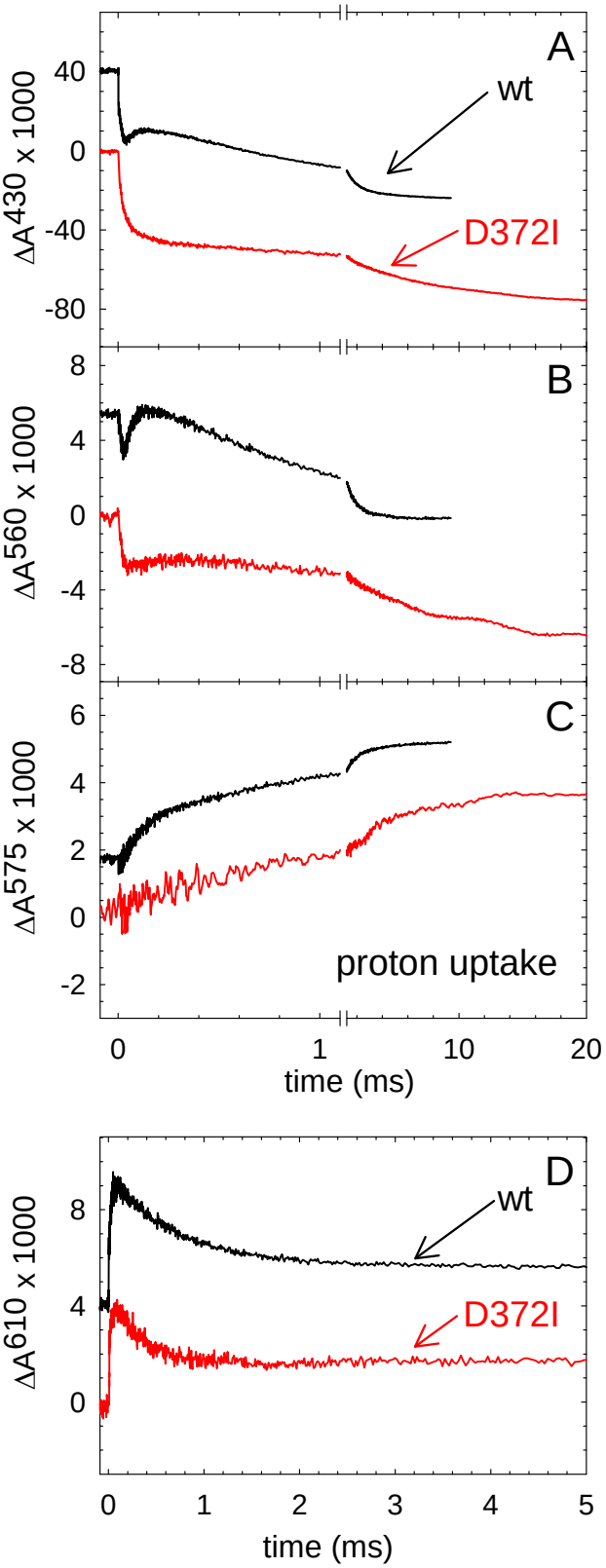
A
wt
D372I
ΔA430 x 1000
40
0
-40
-80
B
ΔA560 x 1000
8
4
0
-4
-8
C
ΔA575 x 1000
6
4
2
0
-2
proton uptake
0
1
10
20
time (ms)
D
wt
D372I
ΔA610 x 1000
8
4
0
0
1
2
3
4
5
time (ms)

Figure 5

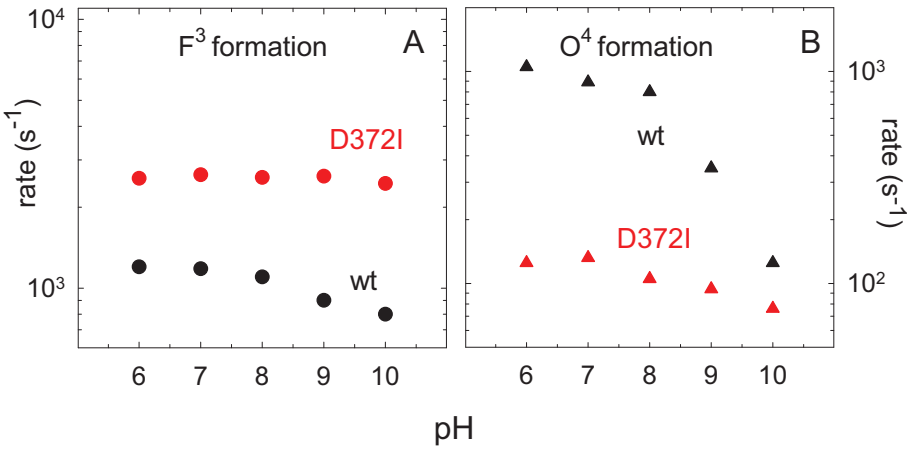
10^4
10^3
rate (s^{-1})
F^3 formation
A
D372I
wt
6
7
8
9
10
pH
O^4 formation
B
10^3
10^2
rate (s^{-1})
wt
D372I

Figure 6

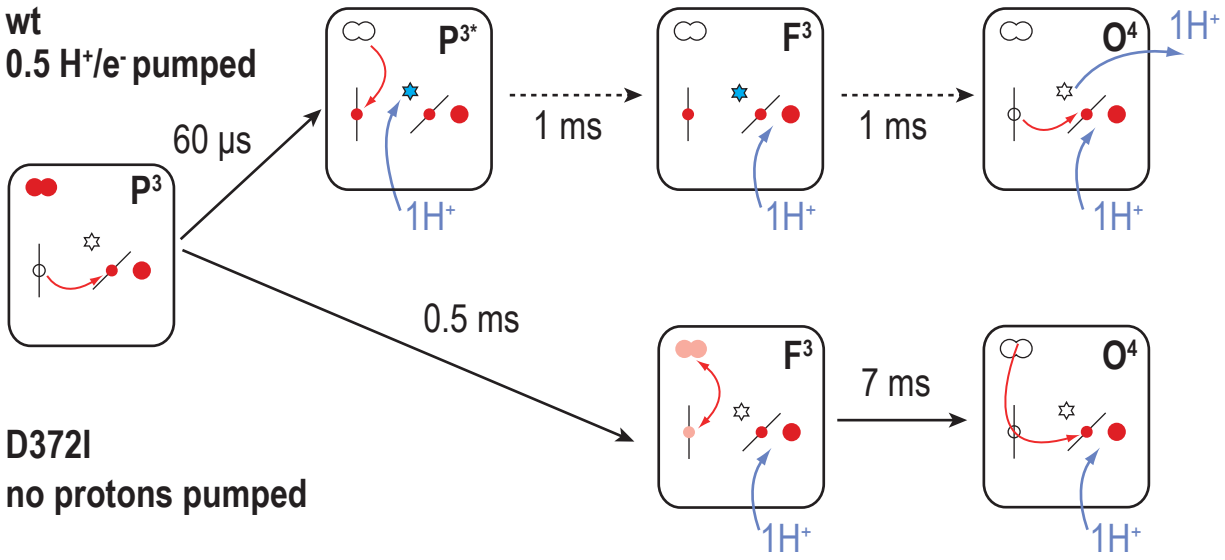
wt
0.5 H+/e- pumped
P3
60 µs
P3*
1H+
1 ms
F3
1H+
1 ms
O4
1H+
1H+
0.5 ms
D372I
no protons pumped
F3
1H+
7 ms
O4
1H+